Electronic Supplementary Information

Self-assembled, robust titanate nanoribbon membranes for highly efficient nanosolid capture and molecule discrimination

Xuebo Cao[*a,b] Yun Zhou,[b] Jun Wu,[b] Yuxin Tang,[c] Lianwen Zhu,[b] and Li Gu[*d]

[a] *School of Biology and Chemical Engineering, Jiaxing University, Jiaxing, Zhejiang 314001, China; E-mail: xbcao@mail.zjxu.edu.cn*

[b] *Key Lab of Organic Synthesis of Jiangsu Province and Department of Chemistry, Soochow University, Suzhou, Jiangsu 215123, China*

[c] *School of Materials Science and Engineering, Nanyang Technological University, Singapore*

[d] *School of Materials and Textile Engineering, Jiaxing University, Jiaxing, Zhejiang, 314001, China; guli@mail.zjxu.edu.cn*

Table S1. Parameters and results for the parallel experiments [a]

Amount of $Ti(OC_4H_9)_4$	Reaction time	TNRs concentration	Morphology of products
0.15 g	48 h	~ 6×10^{-4} g/mL	Discrete TNRs
0.3 g	48 h	~ 1.2×10^{-3} g/mL	Discrete TNRs
0.6 g	48 h	~ 2.2×10^{-3} g/mL	Loose membrane
0.9 g	12 h	~ 3.4×10^{-3} g/mL	Loose membrane
0.9 g	24 h	~ 3.7×10^{-3} g/mL	Loose membrane
0.9 g	36 h	~ 3.8×10^{-3} g/mL	Perfect membrane
0.9 g	48 h	~ 3.8×10^{-3} g/mL	Perfect membrane

[a] TNRs concentration of 2.2×10^{-3} g/mL is required for the occurrence of the self-assembly. And we denote such a concentration as the "supersaturation" concentration of TNRs. As the TNRs concentration is increased to ~ 3.8×10^{-3} g/mL and the reaction time reaches 36 h, perfect and robust membrane will be formed.

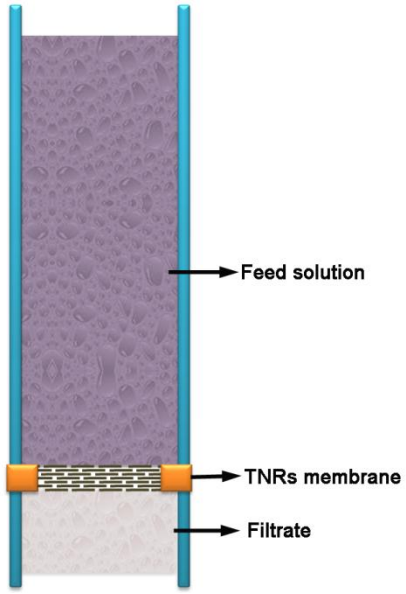

Fig. S1. Schematic illustration of the column-shaped filter apparatus, where the membrane acting as the self-standing permeation barrier is fixed on the bottom of the column by epoxy resin. Owing to the significantly high porosity of the membrane, the permeation of the analytes can be driven by the hydrostatic pressure.

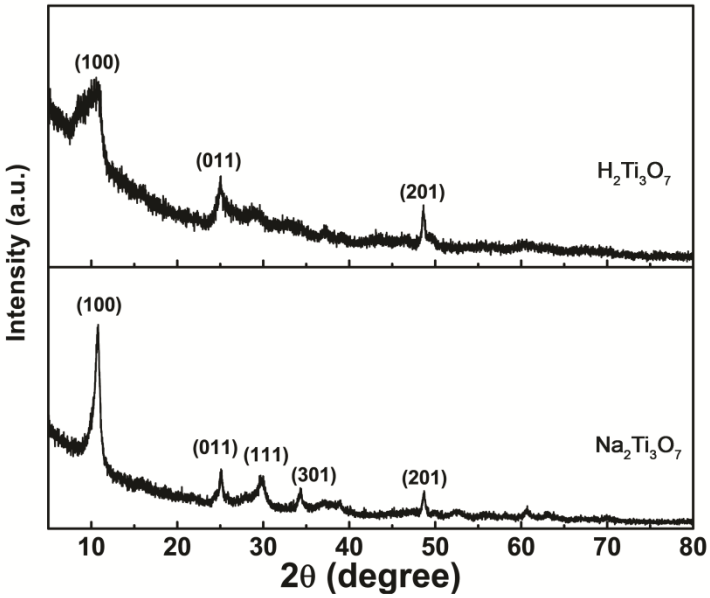

Fig. S2. XRD patterns of the TNRs membranes with the phase of $Na_2Ti_3O_7$ and $H_2Ti_3O_7$.

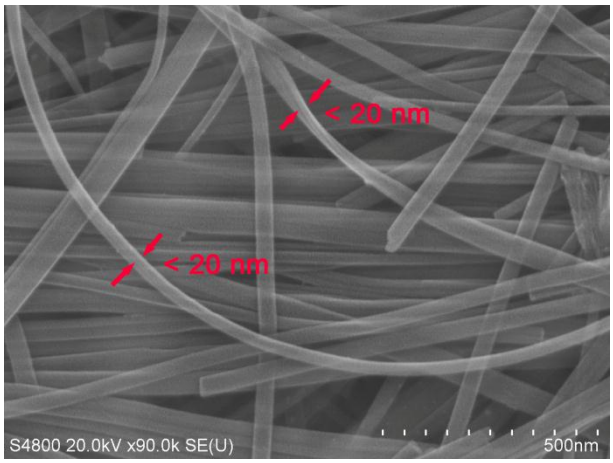

Fig. S3. From the TNRs with side surfaces upwards, we learn that the thickness of the TNRs is less than 20 nm.

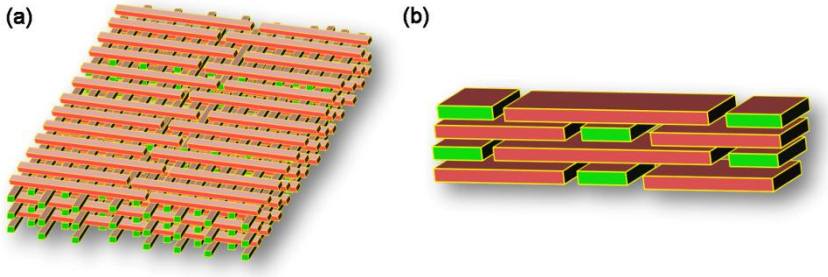

Fig. S4. (a) Schematic profiles of the TNRs membrane. (b) Side view of the membrane. Owing to the flat and broad surfaces, TNRs are able to form interlocked structure.

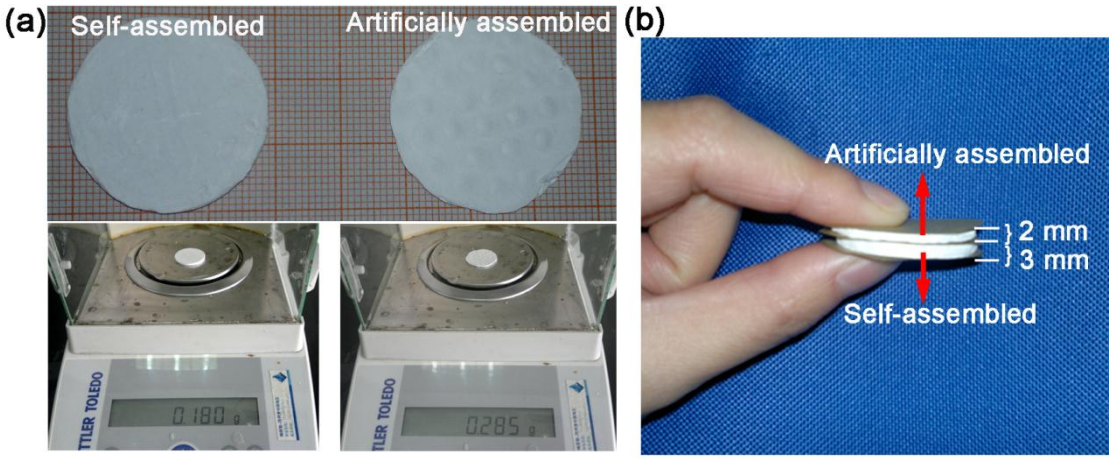

Fig. S5. A Comparison between the self-assembled TNRs membrane and the artificially fabricated TNRs membrane. As shown in Panel a, the artificially fabricated membrane is thinner but much heavier (0.285 g vs. 0.180 g) when compared to the self-assembled ones, indicative of the lower porosity of the former. Further, the artificially fabricated membrane is found to be very fragile.

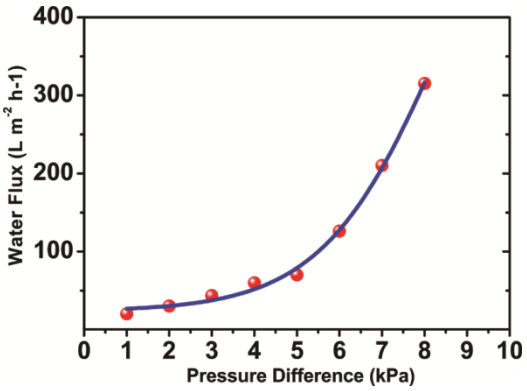

Fig. S6. Measured volume flow of the column-shaped filter apparatus (test liquid: pure water). The pressure difference was provided by the hydrostatic pressure.

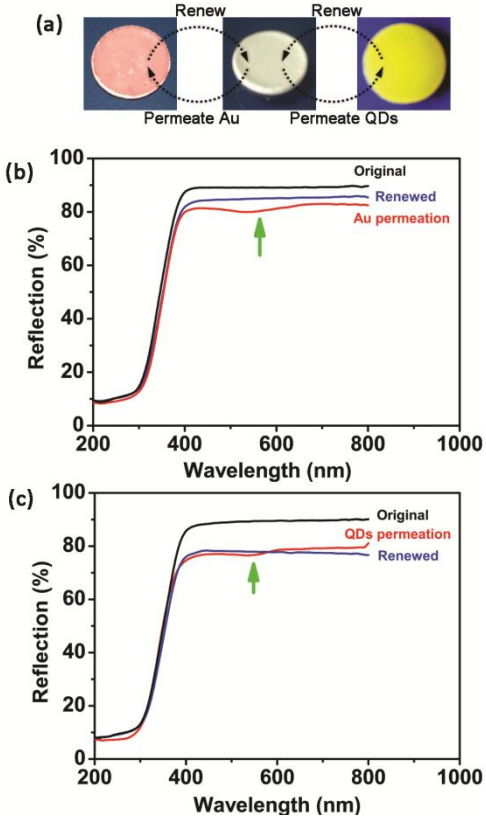

Fig. S7. (a) Photograph shows the permeation-renewal cycles of the TNRs membrane. (b) and (c) Optical reflection spectra of the original TNRs membrane, TNRs membrane capturing 13-nm Au (b) and CdTe QDs (c), and the TNRs membrane after renewal. The arrows indicate the absorption bands of Au nanoparticles (b) and CdTe QDs (c).

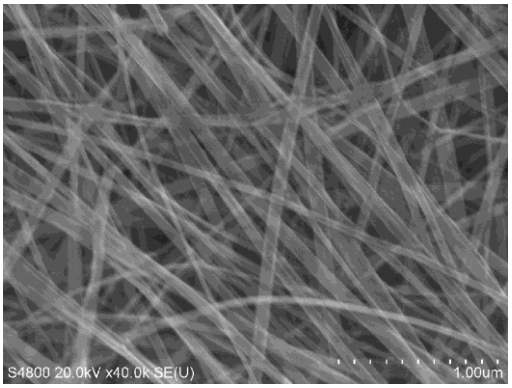

Fig. S8. Au nanoparticles and QDs captured by the TNRs membrane can be dissolved readily and the monolith is returned to its pristine conditions, as indicated by the representative SEM image.

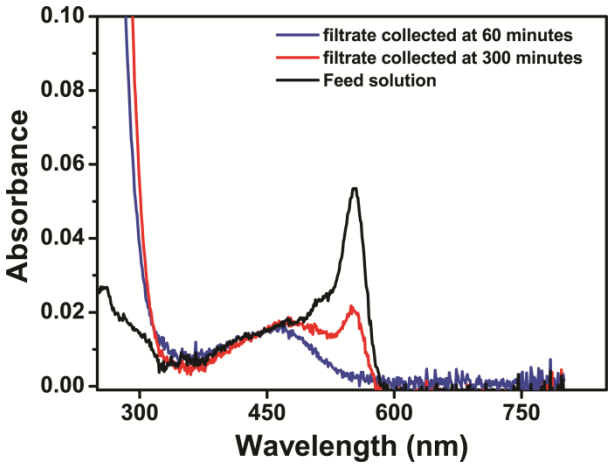

Fig. S9. UV-vis absorption spectra of the original mixed solution of RhB and MO, the filtrate collected at 60 minutes and the filtrate collected at 300 minutes. The characteristic absorption bands for RhB and MO are located at 553 nm and 460 nm, respectively. As seen, there is only a small concentration change for MO in the filtrate and in the feed solution. In contrast, RhB is strongly adsorbed by the TNRs monolith, indicating that the interactions of the TNRs membrane with cationic species and anionic species are different.